

Effects of La_2O_3 on microstructure and wear properties of laser clad $\gamma/\text{Cr}_7\text{C}_3/\text{TiC}$ composite coatings on TiAl intermetallic alloy

Xiu-Bo Liu^{a,b,*}, Rong-Li Yu^c

^a *Laboratory for Laser Intelligent Manufacturing, Institute of Mechanics, Chinese Academy of Sciences, 15 Beisihuanxi Road, Beijing 100080, P.R. China*

^b *School of Materials and Chemical Engineering, Zhongyuan Institute of Technology, 41 Zhongyuan Western Road, Zhengzhou 450007, Henan Province, P.R. China*

^c *School of Materials Science and Engineering, Beihang University, 37 Xueyuan Road, Beijing 100083, P.R. China*

Received 27 March 2005; received in revised form 14 August 2006; accepted 28 August 2006

Abstract

The effects of La_2O_3 addition on the microstructure and wear properties of laser clad $\gamma/\text{Cr}_7\text{C}_3/\text{TiC}$ composite coatings on γ -TiAl intermetallic alloy substrates with $\text{NiCr-Cr}_3\text{C}_2$ precursor mixed powders have been investigated by optical microscopy (OM), scanning electron microscopy (SEM), X-ray diffraction (XRD) and energy-dispersive spectrometer (EDS) and block-on-ring wear tests. The responding wear mechanisms are discussed in detail. The results are compared with that for composite coating without La_2O_3 . The comparison indicates that no evident new crystallographic phases are formed except a rapidly solidified microstructure consisting of the primary hard Cr_7C_3 and TiC carbides and the $\gamma/\text{Cr}_7\text{C}_3$ eutectics distributed in the tough γ nickel solid solution matrix. Good finishing coatings can be achieved under a proper amount of La_2O_3 -addition and a suitable laser processing parameters. The additions of rare-earth oxide La_2O_3 can refine and purify the microstructure of coatings, relatively decrease the volume fraction of primary blocky Cr_7C_3 to $\text{Cr}_7\text{C}_3/\gamma$ eutectics, reduce the dilution of clad material from base alloy and increase the microhardness of the coatings. When the addition of La_2O_3 is approximately 4 wt.%, the laser clad composite coating possesses the highest hardness and toughness. The composite coating with 4 wt.% La_2O_3 addition can result the best enhancement of wear resistance of about 30%. However, too less or excessive addition amount of La_2O_3 have no better influence on wear resistance of the composite coating.

© 2006 Published by Elsevier B.V.

Keywords: TiAl intermetallic alloy; Rare-earth oxide; Microstructure; Wear resistance; Laser cladding

1. Introduction

Because of superior strength-to-weight ratio, high specific modulus and good creep resistance, γ -TiAl intermetallic alloy (hereafter referred as TiAl alloy) is of growing interests for elevated temperature applications in the aerospace, automotive and power generation industries [1–3]. Significant progress has been made in the past decade on improving the room-temperature ductility and high-temperature (>850 °C) oxidation resistance by alloy modifications, processing innovation and surface engineering [4,5]. Some advanced TiAl alloys are now nearly maturing to the stage where it is possible to implement them to the industrial applications. As a new generation of light weight, elevated-temperature candidate structural materials, the tribological

properties need to be enhanced, especially when applied as tribological components such as shafts, blades in gas turbines and exhaust valves in internal combustion engines, in which tribological properties are critically important to the components performance. However, only few reports are available in published literature. Plasma carburization [6] and plasma assisted chemical vapor deposition [7] have been utilized to improve the wear resistance of TiAl alloy by producing Ti_2AlC and TiN thin films, respectively. But all the above fabricated films are too thin (the thickness is about 3–4 μm) to withstand large loads, let alone severe mechanical stress. Laser surface modification is also employed [8–11] to enhance the wear resistance by fabricating in situ wear resistant composite thick coatings (coating thickness up to 1.5 mm) reinforced by TiN and TiC phases. However, both single TiN and TiC phase show poor oxidation-resistance at temperatures higher than 600 °C because of the preferential oxidation of the single TiN and TiC reinforcing phases during high-temperature exposure process. In order to meet the service

* Corresponding author. Tel.: +86 10 62651165; fax: +86 10 62521859.
E-mail address: liubobo0828@yahoo.com.cn (X.-B. Liu).

requirements for TiAl alloy applied as the high-temperature structural components, recently, the authors are exploring new laser surface modification techniques that can noticeably improve the wear- and high-temperature oxidation resistance of the TiAl alloy, simultaneously. The experimental results show that in situ laser surface modification layers that contain both hard wear-resistant reinforcing phases, which can transform into continuous and dense hybrid oxidation scale during the long term high-temperature exposures, can be successfully fabricated on substrate of TiAl alloy with NiCr–Cr₃C₂ mixed precursor alloy powders by laser surface alloying [12] and laser cladding [13]. The addition of rare-earth (RE) in metal materials has multi-functions, such as purification, modification and alloying, thus can improve a series of properties of metal materials to different extent, for example, metallurgy, casting, heat processing, mechanical properties (toughness and low-temperature brittleness). An area of current interest is the modification of RE to surface engineering (wear-, corrosion- and oxidation-resistance). Previous studies have shown the preliminary unique modification effects of RE in surface engineering [14–19]. China has plenty of RE resources, applying RE to the materials surface engineering is a very important aspect of expanding the application field of RE. However, only limited literatures are concerning the modification effects of adding RE on microstructural and tribological characteristics in laser cladding in detail. In this paper, the effects of rare-earth oxide La₂O₃ on the microstructure and wear behaviors of laser clad γ /Cr₇C₃/TiC composite coatings on γ -TiAl intermetallic alloy is studied so as to offer an experimental basis to expand a new promising field of RE.

2. Experimental procedures

The starting experimental material is a commercial titanium aluminides alloy Ti–48Al–2Cr–2Nb (at.%). The TiAl alloy is melted using high purity charge materials by a vacuum magnetic-suspension induction skull melting furnace (100 kW). After repeated melting for three times, each time for 15 min, ingots 40 mm in diameter and 180 mm in length were cast. The as-cast ingots vacuum-sealed in quartz tube were homogenized at 1360 °C for 2 h to produce a fully lamellar microstructure. Specimens of 8 mm × 10 mm × 40 mm for laser surface cladding were cut from the cast and homogenized ingots by electric discharge wire cutting machining.

Experiments of laser surface cladding of the TiAl alloy were conducted on a 5 kW CO₂ laser materials processing systems with 4-axes CNC working station. Specimens, 8 mm × 10 mm × 40 mm in size, were first sandblasted and then cleaned with ethyl alcohol and acetone before laser cladding. Mixed powders of Ni–20 wt.%Cr alloy, 50% weight proportion Cr₃C₂, and La₂O₃, was added into the above mentioned NiCr–50%Cr₃C₂ alloy powders with different weight ratios of 1, 4 and 10%, respectively, were pre-placed on the specimen's surface in thickness of 1.5–2.0 mm. The particle size of the above powders ranges from –100 to 320 mesh. The purity of the above powders is 97, 98 and 99%, respectively. The laser cladding parameters are: laser output power 2.8 kW, beam dimension 1 mm × 18 mm, beam traverse speed 2.0 mm s⁻¹.

Metallographic cross-sections of the laser clad composite coatings were prepared using conventional procedures and are etched with a water solution of HF and HNO₃. Microstructure of the laser clad composite coatings was characterized by OM, SEM and EDS. The phases present in the surface layer are identified by X-ray diffraction method with Cu K α radiation. The recorded intensities were compared with ASTM data. The hardness profile along the coating depth was measured using a microhardness tester with a load of 200 g and a loading time of 10 s.

The room-temperature dry sliding wear test was carried out on a MM-200 block-on-ring wear testing machine as schematically shown in Fig. 1. The load

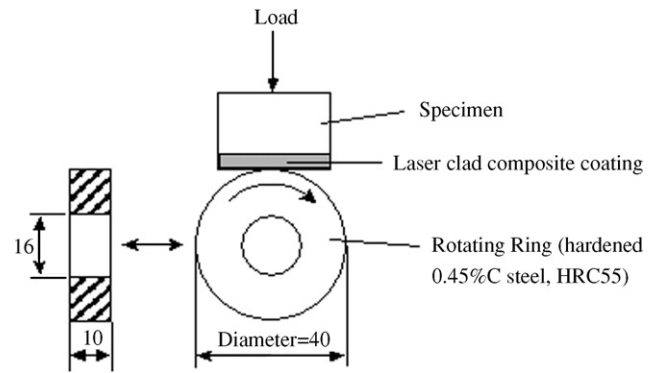


Fig. 1. Schematic of the block-on-ring dry sliding wear tester.

is 98 N. The hardened 0.45% C steel mating ring rotates at 400 rpm which gave a sliding speed of 0.84 m s⁻¹. The complete wear test cycle was 60 min which resulted in a total wear sliding distance of 3.02 × 10³ m. The wear weight loss was measured using a high accuracy photoelectric balance in accuracy of 0.1 mg. The relative wear-resistance (i.e., the ratio of wear weight loss of the original specimen to that of the laser clad specimen) was used to judge the wear resistance of the laser clad coatings. In order to minimize the resulting deviation, three times paralleling experiments had been carried out under each wear test parameters. OM and SEM were also used to characterize the worn surface of the laser clad composite coatings to assist in analyzing the wear mechanisms.

3. Results and discussion

3.1. Microstructure

The results of X-ray diffraction are shown in Fig. 2. As can be seen in Fig. 2(a and b), the addition of 4%La₂O₃ has no significantly influence on the phase constitutions of the laser clad composite coating. Similar to the situation without La₂O₃, an in situ wear-resistant composite coating reinforced by very hard chromium carbide (Cr₇C₃) and titanium carbide (TiC), which distributed uniformly in the tough and corrosion- and oxidation-resistant γ -NiCrAl nickel based solid solution matrix, has been produced on the TiAl alloy substrate.

However, by comparing and analyzing, it can be found that the diffraction angle θ of the coating with La₂O₃ are generally large than that of the coating without La₂O₃. As can be seen in close examination of Fig. 2 and more evidently in Table 1, which shows the diffraction angle θ of stronger diffraction peaks of the coatings.

According to Bragg's law of X-ray diffraction, $2d_{hkl}\sin\theta = \lambda$, where λ is the wavelength of the incident X-ray and is a constant for a certain diffraction condition, d_{hkl} is the interplanar spacing of hkl crystal plane and θ is the diffraction angle. It is obvious that the increase in the diffraction angle θ results in the decrease in interplanar spacing d_{hkl} of crystal plane. The interplanar spacing of crystal plane in cubic system is $d_{hkl} = a/(H^2 + K^2 + L^2)^{1/2}$. The lattice constant a reduces with the decrease in interplanar spacing d_{hkl} for a certain hkl crystal plane. That is to say, the addition of La₂O₃ increases the diffraction angle and decreases interplanar spacing and the lattice constant. As a result, it can be understood theoretically that the microstructure of coatings would be refined when La₂O₃ is added to the coatings.

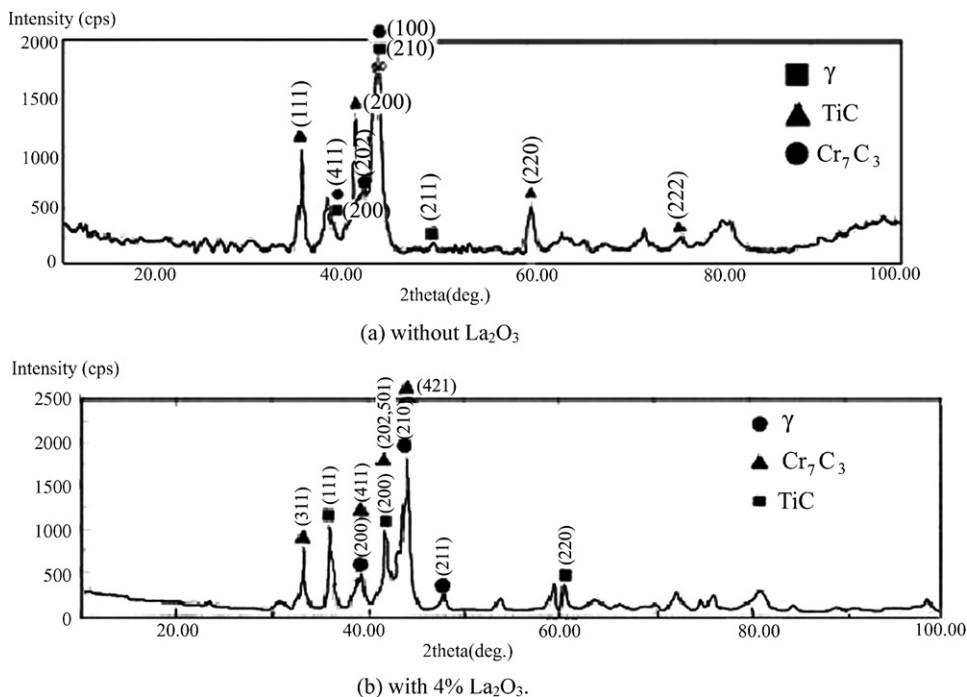


Fig. 2. XRD spectra of the laser clad $\gamma/\text{Cr}_7\text{C}_3/\text{TiC}$ composite coating on TiAl alloy with NiCr–50% Cr_3C_2 precursor mixed powders: (a) without La_2O_3 and (b) with 4% La_2O_3 .

Table 1
Diffraction angle of stronger diffraction peaks

Ingredient	Diffraction angle ($2\theta/\text{degree}$)						
NiCr–50% Cr_3C_2	35.92	37.68	41.82	43.46	60.54	76.12	81.10
NiCr–50% Cr_3C_2 –1.0% La_2O_3	–	–	41.92	44.48	60.98	76.14	82.44
NiCr–50% Cr_3C_2 –4.0% La_2O_3	35.96	38.74	41.76	44.02	60.48	76.22	81.26
NiCr–50% Cr_3C_2 –10.0% La_2O_3	35.96	38.80	42.44	44.14	60.54	76.22	81.50

The microstructure of the coatings is shown in Fig. 3. It can be seen that the main phases in the coating consists of primary blocky wear-resistant Cr_7C_3 and granular TiC and lamellar or chrysanthemum-like $\gamma/\text{Cr}_7\text{C}_3$ eutectics, and the microstructures of coatings are affected greatly by the addition amount of La_2O_3 . Even with 1% La_2O_3 in laser-clad coatings, the appearance of the primary Cr_7C_3 is changed from regular blocky into little clump and global shape, as clearly seen in Fig. 4(a and b). In other words, adding La_2O_3 can hasten the refinement and spheroidization of the primary phase structure. The dimension of the grains is refined from average 5 μm without La_2O_3 to about 3 μm with 1% La_2O_3 (see Fig. 4(a and b)). The addition amount of La_2O_3 affects the microstructural characteristics of all the three phases. With the increasing of the addition amount of La_2O_3 , besides the refined characteristics of the primary Cr_7C_3 , another important feature is the volume fraction of eutectics between the primary phase is noticeably increased, and the morphology of the eutectics is also evidently affected by the addition amount of La_2O_3 . It can be clearly seen by comparing Fig. 4(a) with Fig. 4(d), the morphology of the $\gamma/\text{Cr}_7\text{C}_3$ eutectics is transformed from fine lamellar or chrysanthemum-like without La_2O_3 into distinct flower-like shape with the addition of 10% La_2O_3 .

EDS analysis result of the transition zone between the coating and the substrate is shown in Table 2. It is clear that the element content of Ni, Cr is increasing and Ti, Al is diminishing in the clad coating. Namely, the chemical composition of the clad coating is more approaching to the precursor mixed alloy powders, which indicates that the addition of La_2O_3 can impose beneficial effects on maintaining the clad materials chemical composition and properties and the dilution of clad material from the substrate is evidently decreased, which is of very important meaning for laser cladding.

Synthesizing the above experimental phenomena and analysis and take other literatures [14–19] into account, it can be summarized that effects of La_2O_3 on microstructure of laser-clad coatings are as following: the effects of La_2O_3 in laser-clad

Table 2
Effects of element content of Ni, Cr, Ti and Al in the bonding zone with addition of 4% La_2O_3

	Element content (at.%)			
	Ni	Cr	Ti	Al
Without La_2O_3	1.89	6.15	80.93	3.28
With addition of 4% La_2O_3	14.69	8.10	69.21	2.15

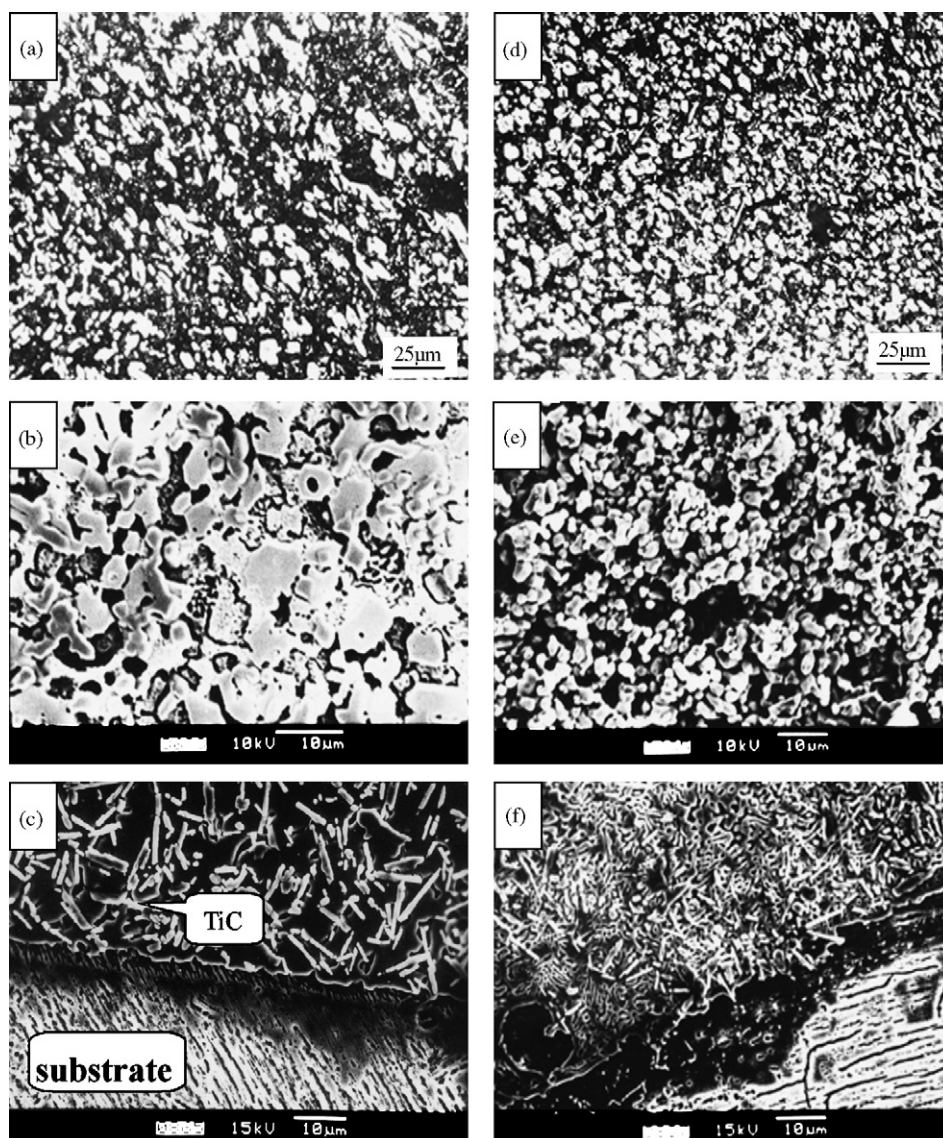


Fig. 3. Micrographs of the laser clad composite coatings without La_2O_3 (a) OM, (b) SEM showing the typical microstructure and (c) SEM showing the bonding zone; (d), (e) and (f) are the counterparts of (a), (b) and (c) with 4% La_2O_3 , respectively.

coatings is similar to that of RE alloy modification reagent in gray cast irons, under the direct radiation of high energy laser beam, most of the La_2O_3 are dissolved and/or decomposed into La ions due to the intense and complicated metallurgical reactions between the alloy elements in the melting-pool, which is evidenced by the obviously enhanced reaction and splashing phenomena of the melting pool, in which, the addition of 10% La_2O_3 shows the remarkable effects. As well known, La is a surface active element with a rather large atomic radius and low electro-negativity. It means that La can form positive ions easily and can react easily with other elements and some stable compounds. During the solidification process of the melting pool, in order to retain the lowest free energy, La in a clad coating would distribute mostly in the front of liquid–solid interface or grain boundary, where the atomic arrangement is irregular [18], thus, increase the tendency of composition super-cooling, therefore, increase the super-cooling degree and nucleation rate, so, the growth of grain will be greatly suppressed. Some un-dissolved

or un-decomposed La_2O_3 itself may become particles of heterogeneous nucleation. It can increase the number of crystal nuclei and hinder the growth of grains during the crystallization of the laser induced melt pool. Therefore, the grain size is noticeably refined. Moreover, the chemical activity of La results in the formation of some high melting point compounds with O, N and S and decreases the melting point of the Ni–Cr–C–Ti–Al multi-alloy system, increases the fluidity of the melting pool during the cladding process. Part of compounds and slag may ascend toward the surface through the molten deposit and remove from the clad layer. Thus, the inclusion content within the coatings is decreased, and the coatings are purified and compacted by deoxidation and desulfuration. Furthermore, La can also reduce surface tension and interfacial energy, thereby decrease critical nucleation work because of their chemical activity. Therefore, the convection of the alloying melting pool is strengthened and the number of nucleation particles increases. So the composition of the fabricated coating may be more uniform and there

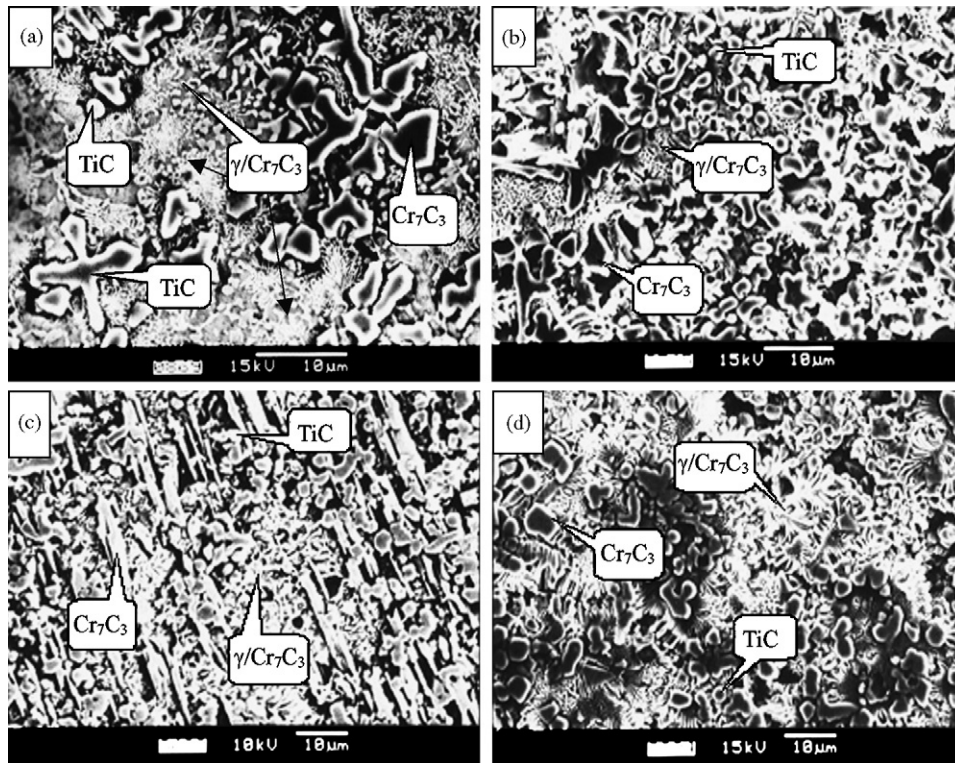


Fig. 4. Micrographs of the coatings with different addition amounts of La_2O_3 showing the refinement and spheroidization of primary Cr_7C_3 and TiC phases and morphology transformation of $\gamma/\text{Cr}_7\text{C}_3$ eutectics: (a) without La_2O_3 , (b) with 1% La_2O_3 , (c) with 4% La_2O_3 and (d) with 10% La_2O_3 .

also exist eutectics in the coating-substrate bonding zone, which is clearly evidenced by Fig. 3(c), in which, intensive formation of TiC without La_2O_3 and Fig. 3(f), in which relatively decreased volume fraction of TiC and increased $\gamma/\text{Cr}_7\text{C}_3$ eutectics with 4% La_2O_3 , can be obviously observed. All the above mentioned factors result in the refinement of the microstructure and purification and compactness of the coatings.

3.2. Profiles of microhardness

The variations of the microhardness of the laser clad composite coatings along depth direction are plotted in Fig. 5. The results show that the addition of La_2O_3 offer higher microhardness values of laser clad coatings. Average microhardness of the coating with 1% La_2O_3 is about the same as that without La_2O_3 , i.e., about HV 650, but the hardness fluctuation is diminished, which implies more uniform microstructure distribution within the whole coating. Different degree of micro-hardness enhancement is achieved in the coatings with 4% La_2O_3 and 10% La_2O_3 addition, in which, the addition of 4% La_2O_3 results in the highest hardness of the coating, i.e., about HV 850. Besides, fluctuation of the micro-hardness within the coating is also the lowest with 4% La_2O_3 . It is easy to understand that the increasing of volume fraction of eutectics means the corresponding decreasing of the content of the primary reinforced phases, as if it would diminish the hardness of the coatings, but the refinement of the primary phase and the increasing of dispersion degree of the eutectics would undoubtedly improve the hardness.

Since the effects of improving the hardness surpass the effects of decreasing the hardness, so the addition of La_2O_3 would bring positive effects on micro-hardness enhancement. When the addition of La_2O_3 is approximately 4 wt.%, the laser clad composite coating possesses the highest hardness and toughness due to the optimal matching of the primary reinforced phase and the relative ductile and tough eutectics, as can be observed in Figs. 3(e) and 4(c).

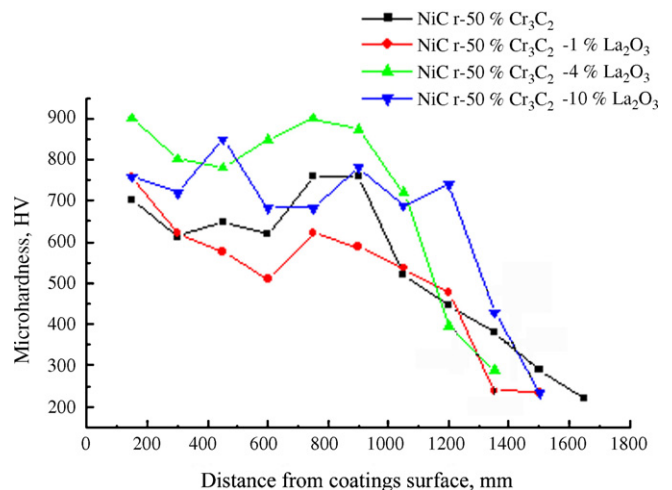


Fig. 5. Microhardness profiles of the laser clad $\gamma/\text{Cr}_7\text{C}_3/\text{TiC}$ composite coatings with $\text{NiCr}-50\%\text{Cr}_3\text{C}_2$ precursor mixed powders and different addition amounts of La_2O_3 .

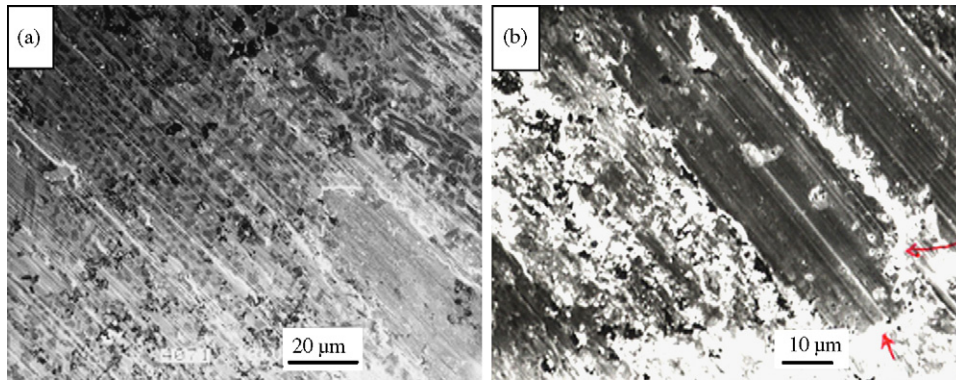


Fig. 6. Worn morphology of (a) laser clad $\gamma/\text{Cr}_7\text{C}_3/\text{TiC}$ composite coating with NiCr–50% Cr_3C_2 and (b) with NiCr–50% Cr_3C_2 –10% La_2O_3 precursor mixed powders.

3.3. Room temperature wear behaviors

The result of room-temperature dry sliding wear resistance is shown in Table 3. It is found that the sliding wear rate of the laser clad coating with approximately 4% La_2O_3 is the lowest for all the testing specimens, which relative sliding wear resistance is about 30% higher than that of without La_2O_3 , but excessive 10% La_2O_3 addition leads to a little decrease of wear resistance. SEM morphologies of the worn surface for the two kinds of laser-clad coatings without and with 10% La_2O_3 addition are shown in Fig. 6. From Fig. 6(a), it can be clearly seen that the primary blocky carbides are playing the outstanding role in resist micro-cutting from the counterpart. Comparing and analyzing Fig. 6(a and b), it is found that worn morphology of the coating with 10% La_2O_3 mainly consists of shallow grooves and plowing traces due to slight abrasive micro-cutting, no spalling and delamination occur. Large white adhesive transfer layer and shallow exfoliating characteristics can be observed in Fig. 6(b), it is most likely to come from the mating counterpart steel. The reason and formation process can be explained as follows: compared to the clad coating, the mating counterpart steel is “soft abrasive” by nature, it can neither press into nor cut the coating effectively, but can only “scratch” the coating very slowly. On the other hand, asperities of the clad coating, which possess high hardness, can both press into and cut the counterpart steel, lead to the formation and transferring of thin films from the counterpart steel to the coating surface, thus, large white adhesive transfer layers are formed after subsequent iterative grinding

and shallow spalling process. The phenomenon that there is no actual wear-resistance increase with the addition of 10% La_2O_3 can be attributed to the following: firstly, the refinement of the microstructure can increase the hardness and toughness of the coatings, meanwhile, the combining-force between the reinforced phases and the γ nickel solid solution matrix is strengthened due to the existence of La in the coatings, therefore, decrease the tendency of cracking and spalling of the reinforced phases during wear process, thus can undoubtedly improve the adhesive and abrasive wear resisting abilities of the coating. On the other hand, since the content of the primary carbides that exert the dominant role in resistant wear is decreasing and the dimension may be over-refined, the excellent wear-resistant abilities of withstanding micro shear cut from micro-roughen peaks of the mating counterpart steel can not be fully brought into play. Thirdly, the excessive La_2O_3 addition would form many inclusions and reduce the microhardness to some extent (see Fig. 5). So there is no actual increase of wear-resistance during the metallic dry sliding wear process because of the above contradictory factors. It also implies that over-refined microstructure is of course beneficial to increase hardness and toughness, but is not helpful to improve wear-resistance by all means. So, it should be emphasized that there exists an optimal addition amount of La_2O_3 , too less or excessive La_2O_3 would not beneficial to improve the microstructure characteristics and wear properties.

4. Conclusions

The addition of rare-earth oxide La_2O_3 in the NiCr– Cr_3C_2 precursor mixed powders leads to obvious refinement and spheroidization of the primary phase of the laser clad composite coatings and relative decrease in volume fraction of primary blocky Cr_7C_3 to $\text{Cr}_7\text{C}_3/\gamma$ eutectics. When the addition of La_2O_3 is approximately 4 wt.%, the laser clad composite coating possesses the highest hardness and toughness. The refinement of the microstructure is beneficial to improve the hardness, strength and toughness of the coatings. The purification and compactness of the coatings is in favor of the wear resistance. All the effects of La_2O_3 on microstructure and wear behaviors are mainly due to the inherent chemical and physical characteristics of La.

Table 3
Relative room temperature wear resistance of the laser clad composite coatings with different addition of La_2O_3 compared to the referential original TiAl alloy

Test materials	Relative wear resistance
Original TiAl alloy	1.00
With NiCr–50% Cr_3C_2 precursor mixed powders	1.90
With NiCr–50% Cr_3C_2 –1% La_2O_3 precursor mixed powders	2.05
With NiCr–50% Cr_3C_2 –4% La_2O_3 precursor mixed powders	2.38
With NiCr–50% Cr_3C_2 –10% La_2O_3 precursor mixed powders	1.90

Acknowledgements

One of the authors (X.-B. Liu) wishes to thank Professor Gang Yu, Dr. Hong-Wei Song and PhD student Ming Pang of the Laboratory for Laser Intelligent Manufacturing, Institute of Mechanics, Chinese Academy of Sciences, for their beneficial discussions.

References

- [1] D.M. Dimiduk, *Mater. Sci. Eng. A* 263 (1999) 281.
- [2] Y.M. Kim, *Acta Metall. Sin.* 12 (4) (1999) 334.
- [3] H.Q. Ye, *Mater. Sci. Eng. A* 263 (1999) 289.
- [4] M. Yoshihara, K. Miura, Y.W. Kim, *TMS* (1995) 93.
- [5] M. Yoshihara, T. Suzuki, R. Tanaka, *ISIJ Int.* 31 (1991) 1201.
- [6] T. Noda, M. Okabe, S. Isobe, *Mater. Sci. Eng. A* 213 (1996) 157.
- [7] D. Xu, Z. Zhang, X. Liu, S. Zou, *Surf. Coat. Technol.* 66 (1994) 486.
- [8] J.A. Vreeling, V. Ocelik, J.T.M. De Hosson, *Acta Mater.* 50 (2002) 4913.
- [9] B.J. Kooi, Y.T. Pei, J.T.M. De Hosson, *Acta Mater.* 51 (2003) 831.
- [10] Y. Chen, H.M. Wang, *Appl. Surf. Sci.* 220 (2003) 186.
- [11] Y. Chen, H.M. Wang, *J. Alloys Compd.* 351 (2003) 304.
- [12] X.-B. Liu, L.-G. Yu, H.-M. Wang, *Rare Met. Mater. Eng.* 30 (3) (2001) 224.
- [13] X.-B. Liu, H.-M. Wang, *Appl. Surf. Sci.* 252 (2006) 5735.
- [14] K.L. Wang, Q.B. Zhang, X.G. Wei, *J. Mater. Sci.* 33 (1998) 3573.
- [15] K.L. Wang, Q.B. Zhang, M.L. Sun, Y.M. Zhu, *Surf. Coat. Technol.* 96 (1997) 267.
- [16] Y. Wang, R. Kovacevic, J.J. Liu, *Wear* 221 (1998) 47.
- [17] K.L. Wang, Q.B. Zhang, M.L. Sun, X.G. Wei, Y.M. Zhu, *Appl. Surf. Sci.* 174 (2001) 191.
- [18] T. Zhao, X. Cai, S.X. Wang, S.A. Zheng, *Thin Solid Films* 379 (2000) 128.
- [19] K.L. Wang, Q.B. Zhang, M.L. Sun, X.G. Wei, *J. Mater. Proc. Technol.* 139 (2003) 448.